Supplementary Material – The Raman signal from a hindered hydrogen rotor

Peter I.C. Cooke[1], Ioan B. Magdău[1,2], Miriam Peña-Alvarez[1], Veronika Afonina[1], Philip Dalladay-Simpson[3], Xiao-Di Liu[4], Ross T. Howie[3], Eugene Gregoryanz[1,3,4] and Graeme J. Ackland[1*]
[1] *CSEC, SUPA, School of Physics and Astronomy, The University of Edinburgh, Edinburgh EH9 3JZ, United Kingdom*
[2] *Department of Chemistry and Chemical Engineering, Caltech, Pasadena, California*
[3] *Center for High Pressure Science and Technology Advanced Research, Shanghai,China and*
[4] *Key Laboratory of Materials Physics, Institute of Solid State Physics, CAS, Hefei, China*

I. INDIRECT CALCULATION OF RAMAN SPECTRA

In section II.D of the main text a method for obtaining the Raman signal from the response of the system to a sudden excitation was presented. A more standard approach is to generate the Raman signal with an 'indirect method'. In this method the Raman signal is considered to be made up of a series of peaks corresponding to each allowed transition in the system. Continuing from eq 21 the polarisability matrix is given by:

$$\Pi_{ij,lml'm'} = \langle lm|\mathbf{R}^T(\theta,\phi)\cdot\boldsymbol{\alpha}\cdot\mathbf{R}(\theta,\phi)|l'm'\rangle \tag{S1}$$

where

$$\boldsymbol{\alpha} = \begin{pmatrix} 1 & 0 & 0 \\ 0 & 1 & 0 \\ 0 & 0 & \alpha \end{pmatrix} \tag{S2}$$

The peak height corresponding to each individual transition is given by:

$$I_{nn'} = \Pi_{nn'}\rho_{nn'} \tag{S3}$$

where

$$\Pi_{nn'} = \sum_{i,j=XY} |\Pi_{ij,nn'}|^2 \tag{S4}$$

for crystallites with c axis parallel to Z or:

$$\Pi_{nn'} = \sum_{i,j=XY} <|\Pi_{ij,nn'}|^2> \tag{S5}$$

where angled brackets indicate a rotational averaging over all θ and ϕ orientations.

with forbidden transitions evaluating to zero. The corresponding Raman shift for each transition is given by:

$$(\nu_{nn'} - \nu_0) = E_{n'} - E_n \tag{S6}$$

To build the overall shape of the spectra the transitions were binned in discrete frequency increments, $\Delta\nu$, and a Lorentzian profile of the form:

$$\phi(\nu) = \frac{I_i \frac{\Gamma}{4\pi^2}}{(\nu-\nu_0)^2 + (\frac{\Gamma}{4\pi})^2} \tag{S7}$$

was overlaid on each bin, where Γ is the same parameter used in eq. 36 and I_i is the sum of all $I_{nn'}$ in frequency bin i.

II. EQQ MEAN FIELD POTENTIAL

A quadrupole-quadrupole potential was generated by assuming that there is only pairwise correlation in the orientations of the H_2 molecules. To generate the potential energy surface the full four-dimensional potential surface was initially calculated for the central rotor in an *hcp* unit cell with each of it's neighbours in turn using the following expression:

$$V_{ij}^{EQQ}(\theta_1,\phi_1,\theta_2,\phi_2) = \frac{\Theta^2}{4\pi\epsilon_0 R_{ij}^5}\Gamma(\theta_1,\phi_1,\theta_2,\phi_2) \tag{S8}$$

Here Θ is the quadrupole moment of the H_2 or D_2 molecule, R_{ij} is the intermolecular separation and Γ is the standard angular dependent term given by:

$$\Gamma(\mathbf{n}_i,\mathbf{n}_j,\hat{\vec{R}}) = \frac{3}{4}[35(\hat{\mathbf{n}}_i\cdot\hat{\vec{R}})^2(\hat{\mathbf{n}}_j\cdot\hat{\vec{R}})^2 - 5(\hat{\mathbf{n}}_i\cdot\hat{\vec{R}})^2$$
$$-5(\hat{\mathbf{n}}_j\cdot\hat{\vec{R}})^2 - 20(\hat{\mathbf{n}}_i\cdot\hat{\vec{R}})(\hat{\mathbf{n}}_j\cdot\hat{\vec{R}})(\hat{\mathbf{n}}_i\cdot\hat{\mathbf{n}}_j) + 2(\hat{\mathbf{n}}_i\cdot\hat{\mathbf{n}}_j)^2 + 1]$$

Where $\mathbf{n}_i$, is the bond orientation vector for molecule i, $\mathbf{n}_j$ is the bond orientation vector for molecule j and $\hat{\vec{R}}$ is the vector from molecule i to molecule j.

A Boltzmann weighted average of the orientations of the second rotor was then taken over θ_2, ϕ_2, giving a two dimensional energy surface:

$$\bar{V}_{ij}^{EQQ}(\theta_1,\phi_1) = \frac{\int V_{ij}^{EQQ}\exp\left\{\frac{-V_{ij}^{EQQ}}{k_BT}\right\}}{Z}\sin\theta_2 d\theta_2 d\phi_2 \tag{S9}$$

where:

$$Z = \int \exp\left\{\frac{-V_{ij}^{EQQ}}{k_b T}\right\} \sin\theta_2 d\theta_2 d\phi_2 \qquad \text{(S10)}$$

Finally the above expression was summed over all pairs to give the molecular field EQQ Potential:

$$V^{M.F.EQQ}(\theta_1, \phi_1) = \sum_{ij} \bar{V}_{ij}^{EQQ}(\theta_1, \phi_1) \qquad \text{(S11)}$$

Surprisingly, this EQQ potential has rather little angular dependence. This is because of the absence of three-body correlations and associated frustration. It implies that in hydrogen EQQ is not strong enough to produce a broken symmetry phase II with a (mean field) single-molecule basis: we note that all candidates for phase II found in DFT have multi-molecular unit cells.

H_2, 10 K		**H_2, 300 K**		**D_2, 10 K**		**D_2, 300 K**	
P (GPa)	r (Å)	P (GPa)	r (Å)	P (GPa)	r (Å)	P (GPa)	r (Å)
6.5	0.742	7.1	0.75	0.6	0.741	7.9	0.741
15.5	0.735	13.4	0.742	2.8	0.734	12.7	0.739
31.1	0.734	19.8	0.741	7.8	0.727	22.2	0.726
45.5	0.721	30.9	0.737	15.9	0.720	32.0	0.723
54.0	0.720	48.3	0.730	21.5	0.720	49.0	0.721

TABLE S1. Fitted bond length scaling in hydrogen at various pressures. Fitted values were limited to within 5% of the gas phase value[1].

H_2, 10 K		**H_2, 300 K**		**D_2, 10 K**		**D_2, 300 K**	
P (GPa)	Γ (cm^{-1})	P (GPa)	Γ (cm^{-1})	P (GPa)	Γ (cm^{-1})	P (GPa)	Γ (cm^{-1})
6.5	137.9	7.1	190.7	0.5	53.1	7.9	144.6
15.5	232.3	13.4	297.8	2.8	70.3	12.7	202.6
31.1	396.8	19.8	406.6	7.8	107.4	22.2	316.5
45.5	225.0	30.9	595.3	15.9	167.5	32.0	434.2
54.0	225.0	48.3	700.00	21.5	209.1	49.0	495.0

TABLE S2. Fitted values for parameter Γ (see eq 36 in main text) for hydrogen and deuterium at 10 K and 300 K.

H_2, 10 K		**D_2, 10 K**	
P (GPa)	o:p	P (GPa)	o:p
5.4	75:25	0.6	70:30
6.5	75:25	2.8	70:30
10.1	75:25	7.8	70:30
15.5	75:25	15.9	80:20
19.3	70:30	21.5	80:20
24.5	65:35	31.8	-
31.1	50:50	40.1	-
35	32:68	48.1	-
45.5	25:75	54.5	-
54	20:80	58.0	-

TABLE S3. *ortho-para* ratios for hydrogen and deuterium fitted to experimental intensities at 10 K. At 300 K the ratio was calculated directly from the temperature (i.e. $T' = T$).

	$\|M_j\| = 1$	$\|M_j\| = 2$	$\|M_j\| = 0$
$S_{c\|\|Z}$	0	12	1
$S_{iso.}$	2	2	1
S_a	2a	12-10a	1

TABLE S4. Fitted *ortho-para* ratios for hydrogen and deuterium at 10 K. At 300 K the ratio was calculated directly from the temperature.

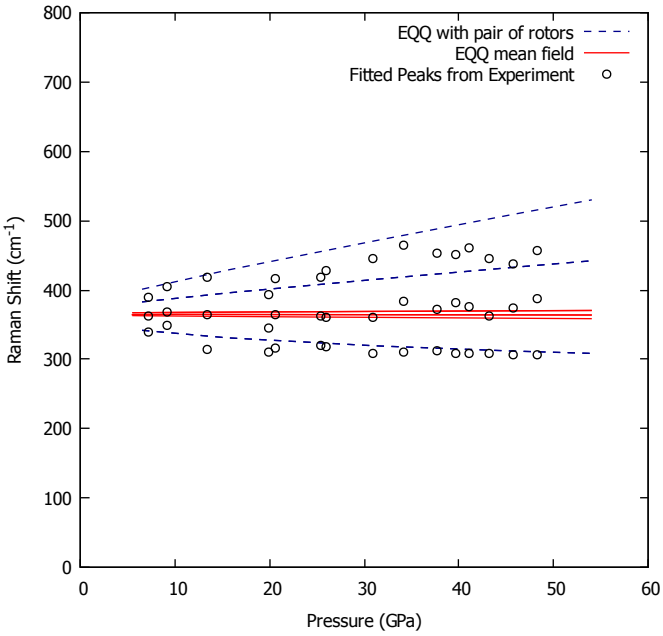

FIG. S1. Frequency shifts for the $S_0(0)$ triplet are shown for the mean field EQQ model (red), the EQQ interaction with a second rotor with a fixed orientation of $\theta = 90, \phi = 0$ (blue dashed) and the least squares fitted experimental peaks (black circles). The mean field only generates small differences in frequency between the $S_0(0)$ contributions, in stark contrast to the fitted shifts from experiment. The quadrupolar interaction with a single rotor at fixed orientation creates a larger difference in frequency between $S_0(0)$ contributions but still shows stark disagreement with experiment at 50 GPa and is not a representative model of the *hcp* crystal in phase I. This demonstrates that while there is sufficient energy in the quadrupole interaction to create the necessary splitting a 'parameter-free' mean field model alone cannot explain the splitting in the $S_0(0)$ triplet, as shown in previous theoretical work on the solid phases of hydrogen.[2]

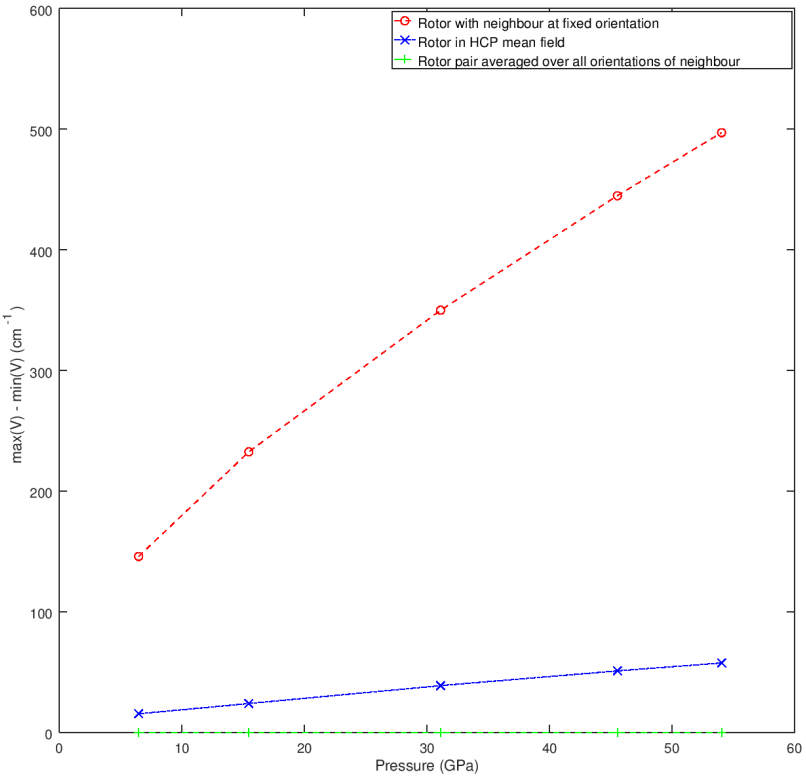

FIG. S2. Difference in energy between the minima and maxima of the potential energy surface for a quadrupole in 3 different cases are shown. A quadrupole with a neighbour of fixed orientation ($\theta = \frac{\pi}{2}, \phi = 0$) is shown in red. A quadrupole in an *hcp* mean field is shown in blue and a quadrupole with a completely uncorrelated neighbour (averaged over all orientations) is shown in green. The mean field shows a reduction of $\sim 95\%$ compared to the a single neighbour at fixed orientation, demonstrating that a parameter free mean field approach is not suitable and hence 3 free parameters were introduced to fit a potential consisting of long range electrostatic interactions and short range steric repulsion.

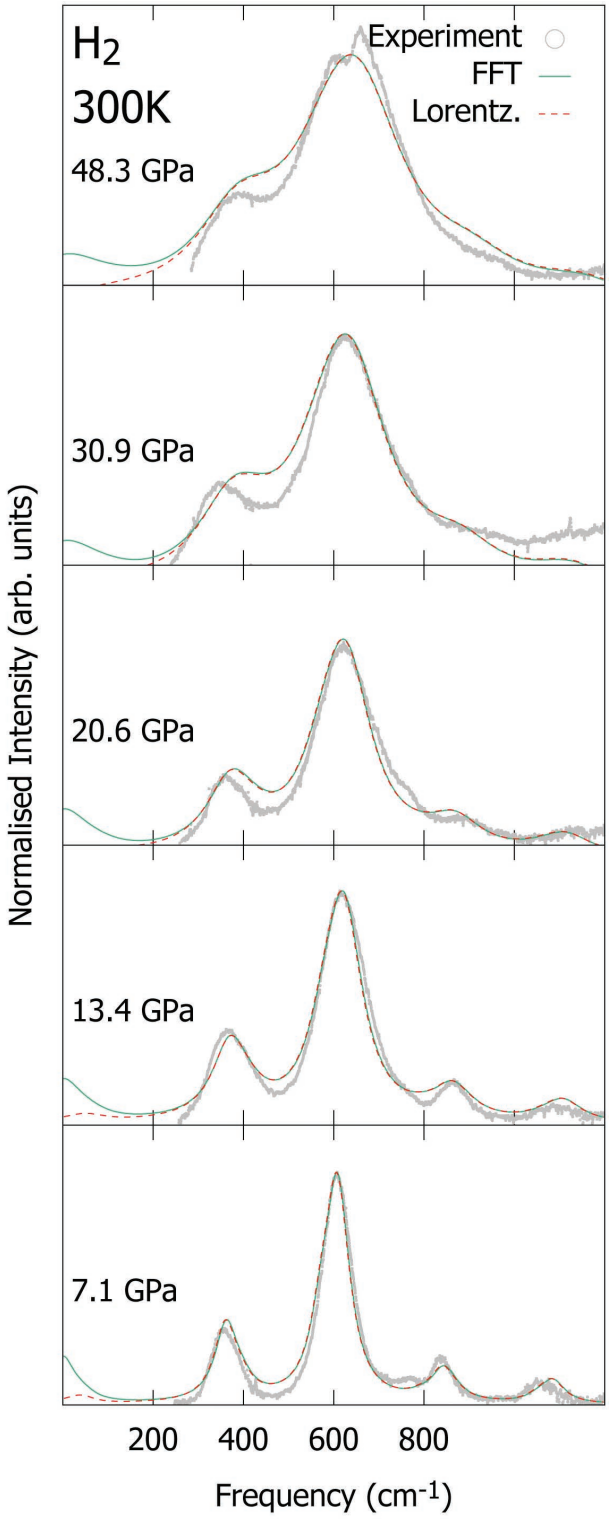

FIG. S3. Calculated Raman spectra using direct (FFT) and indirect (Lorentzians) methods for hydrogen at 300 K. Excellent agreement between both methods can be seen. The divergence seen at low frequencies is due to a different method of filtering out Rayleigh transitions in each method. Perfect agreement could be achieved with a simple adaptation to the Rayleigh filtering method in the FFT approach in future work.

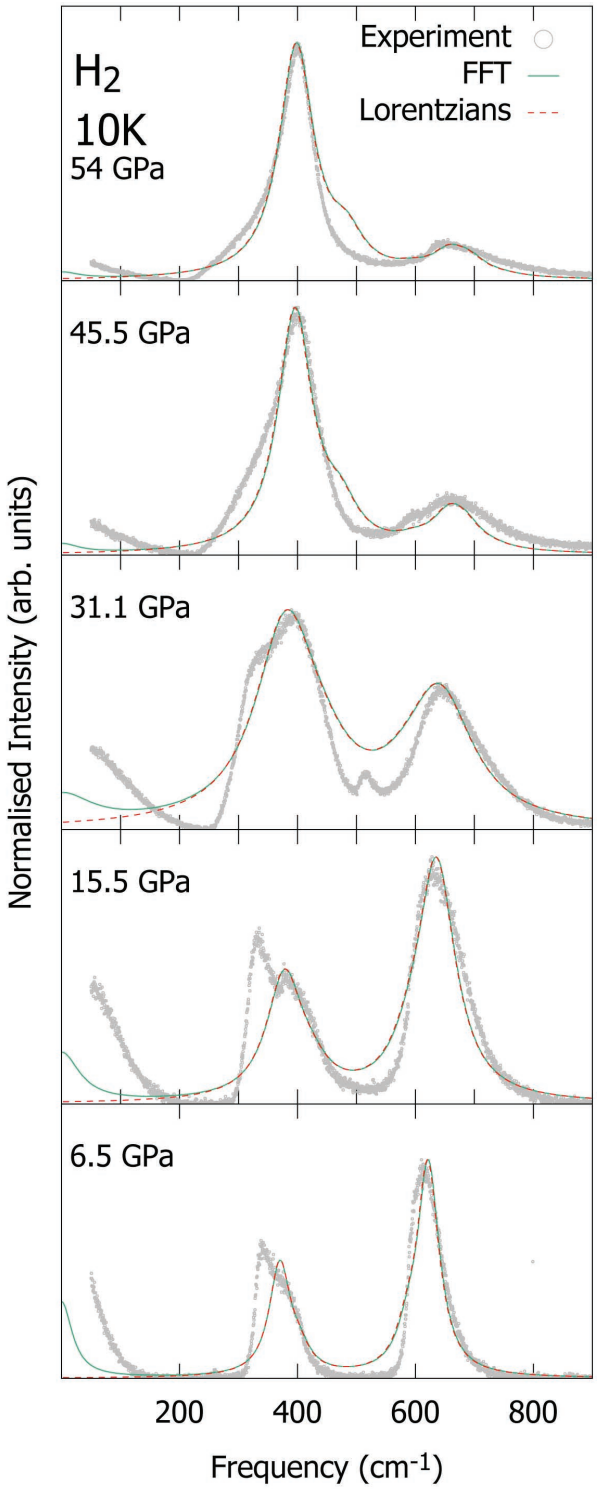

FIG. S4. Calculated Raman spectra using direct (FFT) and indirect (Lorentzians) methods for hydrogen 10 K.

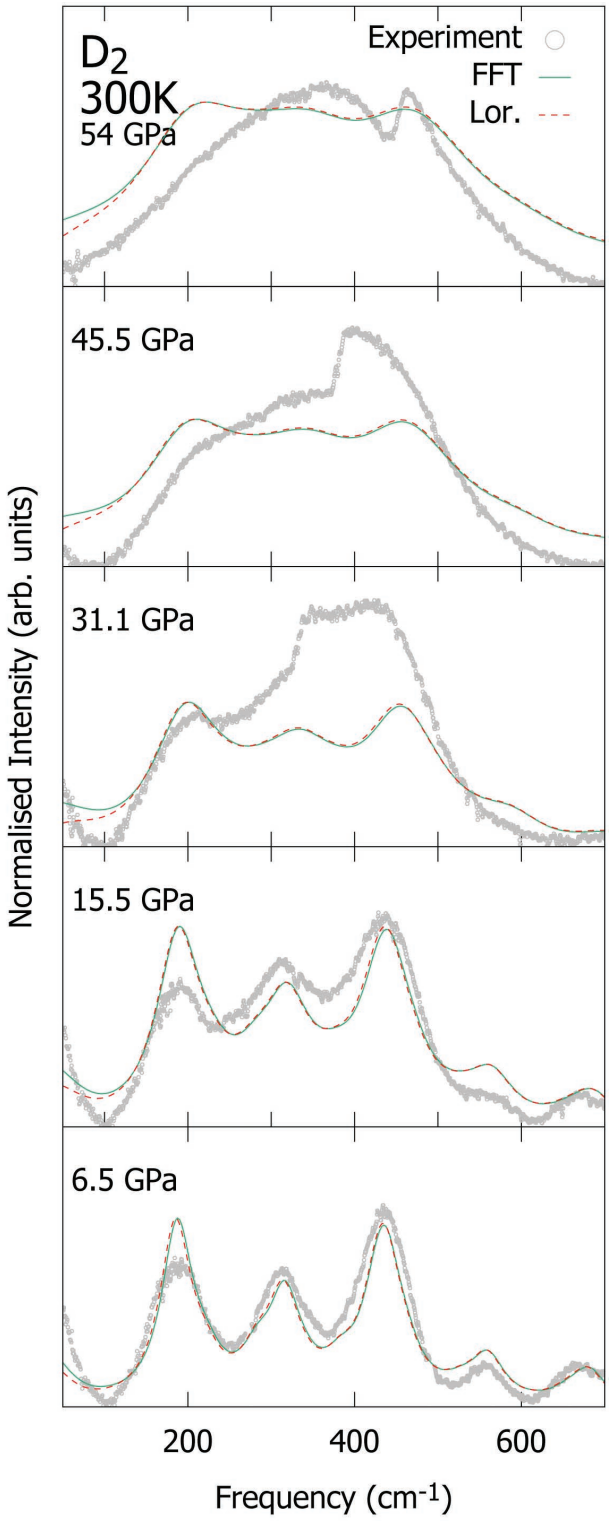

FIG. S5. Calculated Raman spectra using direct (FFT) and indirect (Lorentzians) methods for deuterium at 300 K.

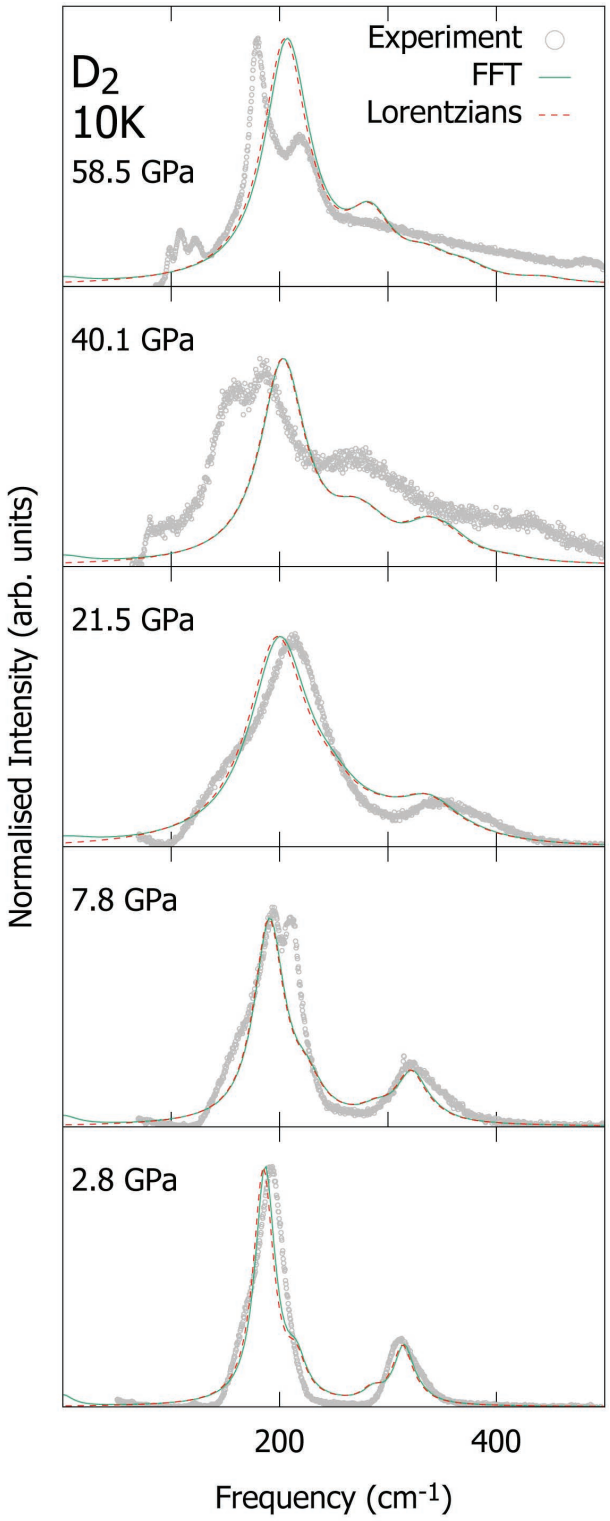

FIG. S6. Calculated Raman spectra using direct (FFT) and indirect (Lorentzians) methods for deuterium at 10 K.

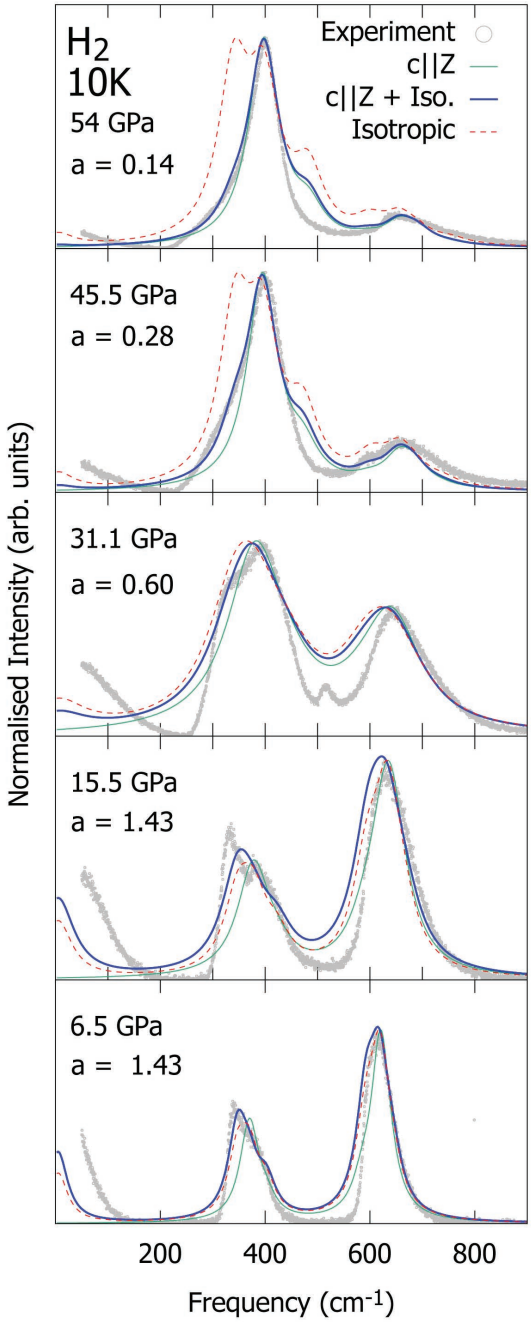

FIG. S7. We also include a signal corresponding to a combination of both geometries (blue). In this case the overall signal, $f(\omega)$, is generated using a weighting parameter 'a' where $f(\omega) = af_{isotropic}(\omega) + (1-a)f_{c||Z}(\omega)$. The signal is much more accurately described by a linear combination of the two geometries at higher spin temperatures i.e. when a higher proportion of *ortho*-hydrogen molecules are present in the sample. The close agreement with experiment achieved here is consistent with the observation that the intensity of the $|M_J| = 1$ peak in the $S_0(0)$ triplet is very well correlated to the abundance of *ortho*-hydrogen as seen in previous experimental studies[3].

.

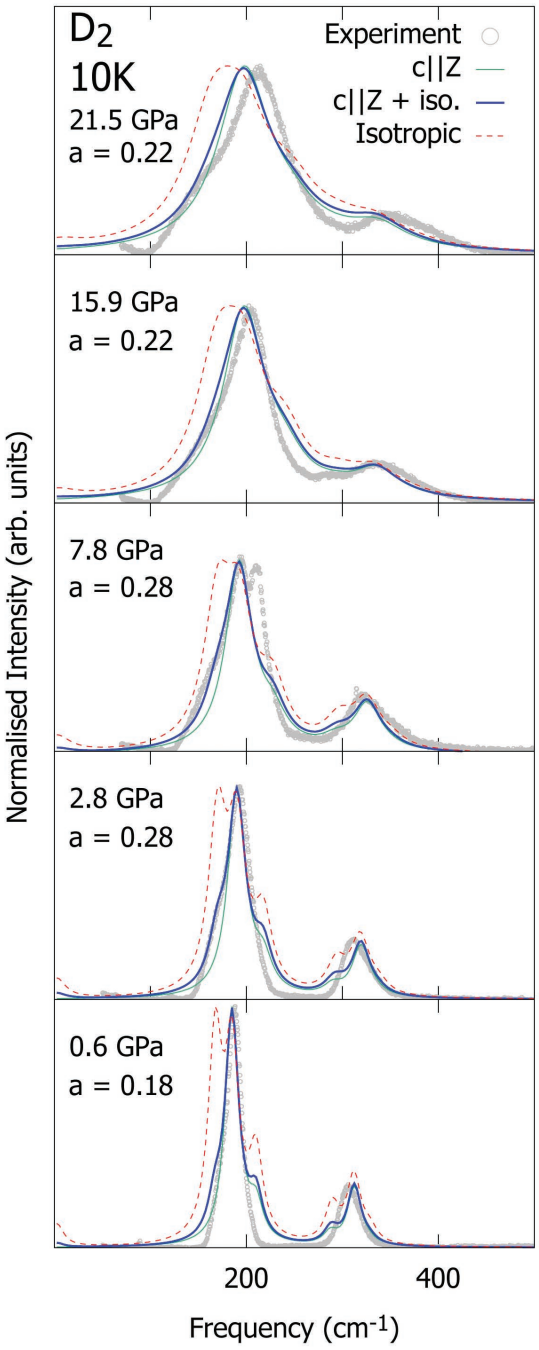

FIG. S8. Deuterium spectra at 10 K, fitted with the procedure described in fig S7. The 'a' parameter shows a much smaller variation with increasing time/pressure with respect to hydrogen. This is consistent with the relatively small change in *ortho*-deuterium fraction compared to hydrogen. (See Table S3)

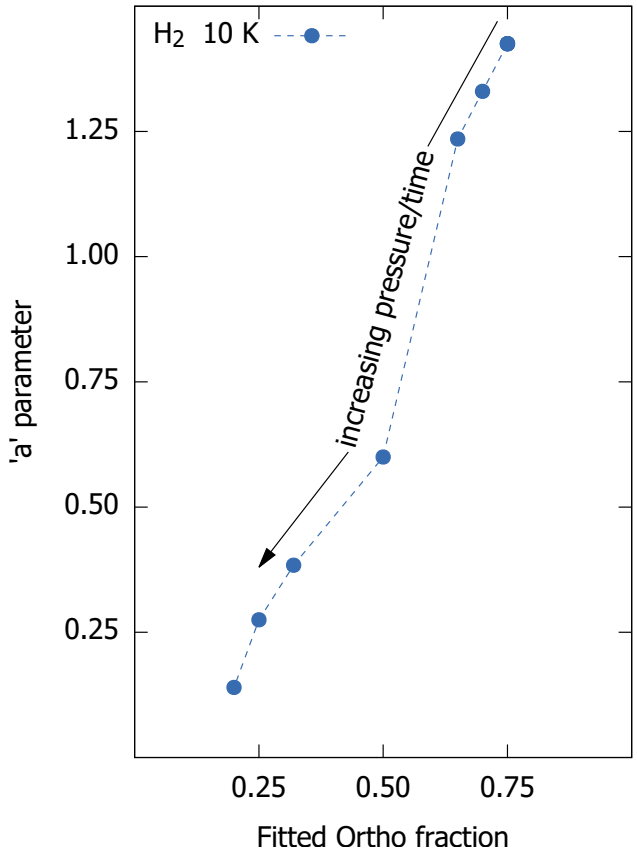

FIG. S9. Variation of the a parameter and the *ortho-para* ratio used to fit the experimental data at 10 K. The *ortho-para* ratio is used to fit the relative peak heights of $S_0(0)$ and $S_0(1)$, corresponding to the occupation of the J=0 and J=1 energy levels. The "a" parameter is a preferred-orientation correction required to fit the $S_0(0)$ peak shape. The strong correlation between the two shows that the "preferred orientation" represents the fact that the M_J=1 component is only visible due to resonant scattering via the *ortho*-peaks. In fact there is always strong alignment with $c||Z$, which means that once the *ortho*-H_2 has converted, the M_J=2 component of $S_0(0)$ is dominant. The *ortho* fraction of 0.75 corresponds to room temperature, and drops to the 10 K equilibrium value as the pressurization proceeds. The calculation suggests that the changing $S_0(0)$ peak shape is mainly due to the *ortho-para* ratio rather than changes in crystal orientations within the cell, or the pressure.

* gjackland@ed.ac.uk

[1] B. Stoicheff, Canadian Journal of Physics **35**, 298 (1957), ISSN 1096083X.
[2] Y. A. Freiman, S. M. Tretyak, H. K. Mao, and R. J. Hemley, Journal of Low Temperature Physics **139**, 765 (2005).
[3] J. H. Eggert, E. Karmon, R. J. Hemley, H.-k. Mao, and A. F. Goncharov, Proceedings of the National Academy of Sciences of the United States of America **96**, 12269 (1999).